



Research article

Numerical approximation of a variable-order time fractional advection-reaction-diffusion model via shifted Gegenbauer polynomials

Yumei Chen^{1,*}, Jijie Zhang² and Chao Pan²

¹ College of Mathematics Education, China West Normal University, Nanchong 637009, China

² School of Mathematics and Information, China West Normal University, Nanchong 637009, China

* **Correspondence:** Email: xhshuxue@163.com.

Abstract: The fractional advection-reaction-diffusion equation plays a key role in describing the processes of multiple species transported by a fluid. Different numerical methods have been proposed for the case of fixed-order derivatives, while there are no such methods for the generalization of variable-order cases. In this paper, a numerical treatment is given to solve a variable-order model with time fractional derivative defined in the Atangana-Baleanu-Caputo sense. By using shifted Gegenbauer cardinal function, this approach is based on the application of spectral collocation method and operator matrices. Then the desired problem is transformed into solving a nonlinear system, which can greatly simplify the solution process. Numerical experiments are presented to illustrate the effectiveness and accuracy of the proposed method.

Keywords: advection-reaction-diffusion equation; variable-order time fractional derivative; Atangana-Baleanu-Caputo derivative; shifted Gegenbauer cardinal function; spectral collocation method

Mathematics Subject Classification: 65N35, 34A08

1. Introduction

With the development of fractional derivative, operators without singular kernel function has become a research topic for the fact that it can better describe nonlocal dynamics systems. Some new classes of them are available including the Caputo-Fabrizio derivative [1], the Atangana-Baleanu derivative [2], etc. See [3–9] and references therein for further details. On the other hand, it is worth noting that the fractional calculus has extended to study the variable-order (VO) models [10, 11], which are generalizations of fixed-order fractional derivatives. For example, some VO fractional differential diffusion processes can better simulate the temperature change than integer order classical models.

Many numerical treatments have recently been proposed to approximate VO fractional differential equations. VO fractional derivatives are global operators in essence, it is more convenient to use global technology such as spectral methods to deal with VO operators [12]. Spectral methods can obtain the desired solutions with a small degree of freedom, which makes improved accuracy with a significant reduction in the computational cost [13]. Here, we focus on the polynomial-based spectral collocation methods. Lagrange polynomials were applied to simulate two chaotic practice problems modeled by VO fractional differential equations [14]. A collocation technique based on a reproducing kernel function was developed for VO fractional initial value problems and terminal value problems [15]. Shifted Jacobi polynomials were used to approximate VO time fractional Emden-Fowler equation [16], two-dimensional VO time fractional cable equations [17]. Gegenbauer polynomials are a special of Jacobi polynomials. As a significant kind of orthogonal polynomials, Gegenbauer polynomials are the generalization of Legendre polynomials and Chebyshev polynomials, which have been widely used in mathematical physics, engineering technology, scientific computing and other fields. Shifted Gegenbauer operational matrices jointly with the Tau method were developed for solving fractional differential equations [18]. Shifted Gegenbauer polynomials were applied to solve time-fractional delay differential equations [19]. Fractional optimal control problems were solved via Gegenbauer cardinal functions [20]. A numerical scheme in [21] was proposed to solve the nonlinear VO fractional Schrödinger equation by using the shifted Legendre polynomials.

Diffusion process is one of the most famous processes in nature, such as the numerical simulation of urban air quality [22], transport process of pollutants in groundwater [23], numerical determination the pollution sources in a river [24], transport process of bimolecular reaction in porous media [25]. The fractional form of diffusion equation can model the random collision of solute molecules with fluid molecules causes diffusion and produces fluxes from high concentrated to low concentration regions. Numerical solutions of space fractional diffusion equation defined by Caputo derivative were obtained via shifted Gegenbauer polynomials [26]. A compact implicit difference scheme was proposed to approximate time-fractional diffusion-wave equation [27]. An operational matrix was derived for multidimensional VO time fractional anomalous diffusion equations based on the shifted Chebyshev collocation methods [28]. Gegenbauer spectral method was used to approximate convection-diffusion equation with time fractional derivative [29]. By using the shifted Chebyshev polynomial of the second kind as the cardinal function, an operational matrix scheme was given in [30] for approximating VO time fractional nonlinear reaction-diffusion equation. A homotopy perturbation method was applied for time fractional advection-reaction-diffusion equation with Liouville-Caputo derivative [31]. A numerical method was proposed to approximate time fractional advection-reaction-diffusion equation by using shifted Legendre polynomials [32].

Given the following VO time-fractional derivative model for advection-reaction-diffusion equation

$$\begin{cases} \frac{\partial^{\theta(\sigma,\tau)} u(\sigma,\tau)}{\partial \tau^{\theta(\sigma,\tau)}} = \kappa \frac{\partial^2 u(\sigma,\tau)}{\partial \sigma^2} - \mu \frac{\partial u(\sigma,\tau)}{\partial \sigma} + \delta(\sigma, \tau, u(\sigma, \tau)) + f(\sigma, \tau), & (\sigma, \tau) \in [0, X] \times [0, T], \\ u(\sigma, 0) = g(\sigma), \\ u(0, \tau) = h_1(\tau), \quad u(X, \tau) = h_2(\tau). \end{cases} \quad (1.1)$$

Here, σ and τ represent spatial and time nodes respectively, $u(\sigma, \tau)$ is concentration of the solute in fluid at finite distance, parameters κ and μ are the constant coefficients on \mathbb{R} . Variable order $\theta(\sigma, \tau) \in C(0, 1)$, $\delta(\sigma, \tau, u(\sigma, \tau))$ and $f(\sigma, \tau)$ are continuous nonlinear source terms.

This paper aims to investigate numerically problem (1.1) with Atangana-Baleanu-Caputo defined

time-fractional derivative without singular kernel [2]. For solving Eq (1.1), the Gegenbauer spectral method will be used. Firstly, the considered model is approximated by the shifted Gegenbauer polynomials (SGPs) with undetermined coefficients. A nonlinear algebraic equations are derived via the SGPs operational matrices by choosing suitable collocation points. Finally, the desired problem is transformed into solving the obtained nonlinear system.

This work proceeds as follows. Preliminaries on variable-order fractional derivatives with Mittag-Leffler kernel are provided in Section 2. Review of some useful properties of the SGPs is presented in Section 3. The operational matrices of cardinal functions for the SGPs are obtained in Section 4. Based on the Gegenbauer spectral method, the proposed numerical scheme is formulated in Section 5. A few illustrative examples with different initial conditions and boundary conditions are shown in Section 6. The last section is devoted to a brief conclusion.

2. Variable order fractional calculus with Mittag-Leffler kernel

This section devotes to some useful preliminaries of Atangana-Baleanu-Caputo (ABC) derivatives with fractional order. To begin with we introduce the Mittag-Leffler function $\mathbf{E}_{\alpha_1, \alpha_2}(\tau)$ that will commonly be encountered in fractional calculus as follows [33].

$$\mathbf{E}_{\alpha_1, \alpha_2}(\tau) = \sum_{j=0}^{\infty} \frac{\tau^j}{\Gamma(j\alpha_1 + \alpha_2)}, \quad \tau \in \mathbb{C}, \quad \alpha_1, \alpha_2 \in \mathbb{R}^+. \quad (2.1)$$

Notation $\mathbf{E}_{\alpha_1}(\tau)$ is used for $\alpha_2 = 1$. Where $\Gamma(\cdot)$ is the Gamma function and $\Gamma(x) = (x-1)!$ if $x \in \mathbb{Z}^+$. The relationship between the Gamma function and the Beta function is

$$\mathbf{B}(p, q) = \int_0^1 t^{p-1}(1-t)^{q-1} dt = \frac{\Gamma(p)\Gamma(q)}{\Gamma(p+q)}, \quad p, q \in \mathbb{R}^+. \quad (2.2)$$

The definition of the ABC fractional derivative for the order $\bar{\theta}$ is given by

$$\frac{\partial^{\bar{\theta}} u(\sigma, \tau)}{\partial \tau^{\bar{\theta}}} = \frac{\bar{\mathbf{C}}(\bar{\theta})}{1-\bar{\theta}} \int_0^{\tau} \frac{\partial u(\sigma, s)}{\partial s} \mathbf{E}_{\bar{\theta}} \left(\frac{-\bar{\theta}(\tau-s)^{\bar{\theta}}}{1-\bar{\theta}} \right) ds, \quad 0 < \bar{\theta} < 1, \quad (2.3)$$

where $\mathbf{C}(\bar{\theta})$ is a normalization function taking the form

$$\bar{\mathbf{C}}(\bar{\theta}) = 1 - \bar{\theta} + \frac{\bar{\theta}}{\Gamma(\bar{\theta})}.$$

The definition of the ABC fractional derivative in the sense of variable order $\theta(\sigma, \tau)$ is given by

$$\frac{\partial^{\theta(\sigma, \tau)} u(\sigma, \tau)}{\partial \tau^{\theta(\sigma, \tau)}} = \frac{\mathbf{C}(\theta(\sigma, \tau))}{1-\theta(\sigma, \tau)} \int_0^{\tau} \frac{\partial u(\sigma, s)}{\partial s} \mathbf{E}_{\theta(\sigma, \tau)} \left(\frac{-\theta(\sigma, \tau)(\tau-s)^{\theta(\sigma, \tau)}}{1-\theta(\sigma, \tau)} \right) ds, \quad (2.4)$$

where $\mathbf{C}(\theta(\sigma, \tau)) = 1 - \theta(\sigma, \tau) + \frac{\theta(\sigma, \tau)}{\Gamma(\theta(\sigma, \tau))}$ is a normalization function, and $u(\sigma, \tau) \in C^1([0, X] \times [0, T])$ is a real function.

Corollary 2.1. ([34]) Let $k \in \mathbb{N} \cup \{0\}$, there is

$$\frac{\partial^{\theta(\sigma, \tau)} \tau^k}{\partial \tau^{\theta(\sigma, \tau)}} = \begin{cases} 0, & k = 0, \\ \frac{\mathbf{C}(\theta(\sigma, \tau)) k! \tau^k}{1-\theta(\sigma, \tau)} \mathbf{E}_{\theta(\sigma, \tau), k+1} \left(\frac{-\theta(\sigma, \tau) \tau^{\theta(\sigma, \tau)}}{1-\theta(\sigma, \tau)} \right), & k = 1, 2, \dots \end{cases} \quad (2.5)$$

3. The shifted Gegenbauer polynomials and their properties

Given a closed interval $[0, T]$, we use the shifted Gegenbauer polynomials (SGPs) of order m as the cardinal function [35], which is denoted by $G_{T,m}^\lambda(\tau)$. It is defined by

$$G_{T,m}^\lambda(\tau) = \frac{\Gamma(\lambda + 0.5)}{\Gamma(2\lambda)} \sum_{k=0}^m \frac{(-1)^{k+m} \Gamma(2\lambda + k + m)}{k!(m-k)! \Gamma(k + \lambda + 0.5)} \left(\frac{\tau}{T}\right)^k, \quad m \in \mathbb{Z}^+, \lambda \text{ is a constant}, \quad (3.1)$$

with the orthogonal property

$$\int_0^T G_{T,m}^\lambda(\tau) G_{T,n}^\lambda(\tau) w_T^\lambda(\tau) d\tau = h_{T,m}^\lambda \delta_{mn}. \quad (3.2)$$

In Eq (3.2), the weight function is $w_T^\lambda(\tau) = (T - \tau)^{\lambda-0.5} \tau^{\lambda-0.5}$ and

$$h_{T,m}^\lambda = \frac{2^{1-4\lambda} T^{2\lambda} \Gamma(m + 2\lambda) \pi}{(m + \lambda) m! \Gamma^2(\lambda)}. \quad (3.3)$$

If $u(x) \in L^2[0, T]$, then it can be approximated by a polynomial u_p of order p in terms of the SGPs

$$u(\tau) \simeq u_p(\tau) = \sum_{m=0}^p c_m G_{T,m}^\lambda(\tau), \quad (3.4)$$

with the coefficients c_m are determined by the orthogonality condition

$$c_m = \frac{1}{h_{T,m}^\lambda} \int_0^T w_T^\lambda(\tau) u(\tau) G_{T,m}^\lambda(\tau) d\tau, \quad m = 0, 1, \dots, p. \quad (3.5)$$

Let

$$C = [c_0, c_1, \dots, c_p]^T, \quad \Psi_{T,p}(\tau) = [G_{T,0}^\lambda(\tau), G_{T,1}^\lambda(\tau), \dots, G_{T,p}^\lambda(\tau)], \quad (3.6)$$

then Eq (3.4) is expressed in matrix form as

$$u(\tau) \simeq u_p(\tau) \triangleq C^T \Psi_{T,p}(\tau). \quad (3.7)$$

Likewise, the function $u(\sigma, \tau) \in L^2([0, T] \times [0, T])$ with two variables can be approximated by the double SGPs of degrees q and p as

$$u(\sigma, \tau) \simeq u_{q,p}(\sigma, \tau) = \sum_{m=0}^q \sum_{n=0}^p u_{mn} G_{X,m}^\lambda(\sigma) G_{T,n}^\lambda(\tau) \triangleq \Psi_{X,q}(\sigma)^T U \Psi_{T,p}(\tau), \quad (3.8)$$

where $U = [u_{mn}]$ is a $(q + 1) \times (p + 1)$ unknown coefficients matrix with

$$u_{mn} = \frac{1}{h_{X,m-1}^{(a,b)} h_{T,n-1}^{(a,b)}} \int_0^X \int_0^T w_X^\lambda(\sigma) w_T^\lambda(\tau) u(\sigma, \tau) G_{X,m-1}^\lambda(\sigma) G_{T,n-1}^\lambda(\tau) d\tau d\sigma,$$

for $m = 1, 2, \dots, q + 1, n = 1, 2, \dots, p + 1$.

4. Operational matrices

In this section, some novel operator matrices about the SGPs are derived. Let

$$\Phi_p(\tau) = [\varphi_{p,0}(\tau), \varphi_{p,1}(\tau), \dots, \varphi_{p,p}(\tau)]^T, \quad \text{with } \varphi_{p,m}(\tau) = \tau^m \quad (m = 0, 1, \dots, p). \quad (4.1)$$

Lemma 4.1. *The basis vector $\Psi_{T,p}(\tau)$ in (3.6) satisfies*

$$\Phi_p(\tau) = \Theta_{T,p} \Psi_{T,p}(\tau), \quad (4.2)$$

where the transform matrix $\Theta_{T,p} = [\xi_{T,mn}]$ is an $(p+1)$ -order square matrix with

$$\begin{aligned} \xi_{T,mn} &= \frac{2^{4\lambda-1} T^{m-3} (n+\lambda-1)(n-1)! \Gamma(\lambda+0.5) \Gamma^2(\lambda)}{\pi \Gamma(n+2\lambda-1)} \\ &\times \sum_{k=0}^{n-1} (-1)^{k+n-1} \frac{\Gamma(2\lambda+k+n-1) \Gamma(\lambda+k+m-0.5)}{k!(n-k-1)! \Gamma(\lambda+k+0.5) \Gamma(2\lambda+k+m)}, \quad 1 \leq m, n \leq p+1. \end{aligned}$$

Proof. By expressing the element $\varphi_{p,\hat{m}}(\tau)$ ($\hat{m} = 0, 1, \dots, p$) of $\Phi_p(\tau)$ in terms of the SGPs, we have

$$\varphi_{p,\hat{m}}(\tau) = \sum_{\hat{n}=0}^p \hat{\xi}_{T,\hat{m}\hat{n}} G_{T,\hat{n}}^\lambda(\tau) \triangleq \hat{\Theta}_{T,\hat{m}}^T \Psi_{T,p}(\tau), \quad (4.3)$$

where

$$\hat{\Theta}_{T,\hat{m}}^T = [\hat{\xi}_{T,\hat{m}0}, \hat{\xi}_{T,\hat{m}1}, \dots, \hat{\xi}_{T,\hat{m}p}].$$

Eq (3.5) yields

$$\hat{\xi}_{T,\hat{m}\hat{n}} = \frac{1}{h_{T,\hat{n}}^\lambda} \int_0^T w_T^\lambda(\tau) \varphi_{p,\hat{m}}(\tau) G_{T,\hat{n}}^\lambda(\tau) d\tau, \quad 0 \leq \hat{n} \leq p. \quad (4.4)$$

By recalling that $w_T^\lambda(\tau) = (T-\tau)^{\lambda-0.5} \tau^{\lambda-0.5}$ and using Eqs (3.1), (3.3) and (4.1), we get

$$\begin{aligned} \hat{\xi}_{T,\hat{m}\hat{n}} &= \frac{(\hat{n}+\lambda)\hat{n}! \Gamma^2(\lambda)}{2^{1-4\lambda} T^{2\lambda} \Gamma(\hat{n}+2\lambda) \pi} \int_0^T (T-\tau)^{\lambda-0.5} \tau^{\lambda-0.5} \tau^{\hat{m}} d\tau \\ &\times \frac{\Gamma(\lambda+0.5)}{\Gamma(2\lambda)} \sum_{k=0}^{\hat{n}} \frac{(-1)^{k+\hat{n}} \Gamma(2\lambda+k+\hat{n})}{k!(\hat{n}-k)! \Gamma(k+\lambda+0.5)} \left(\frac{\tau}{T}\right)^k \\ &= \frac{(\hat{n}+\lambda)\hat{n}! \Gamma^2(\lambda)}{2^{1-4\lambda} T^{2\lambda} \Gamma(\hat{n}+2\lambda) \pi} \sum_{k=0}^{\hat{n}} \frac{(-1)^{k+\hat{n}} \Gamma(2\lambda+k+\hat{n})}{k!(\hat{n}-k)! \Gamma(k+\lambda+0.5) T^k} I_\tau, \end{aligned} \quad (4.5)$$

where $I_\tau = \int_0^T (T-\tau)^{\lambda-0.5} \tau^{\lambda+\hat{m}+k-0.5} d\tau$.

Let $\tau = Tx$ and from (2.2), it is

$$\begin{aligned} I_\tau &= T^{2\lambda+\hat{m}+k-2} \int_0^1 x^{\lambda+\hat{m}+k-0.5} (1-x)^{\lambda-0.5} dx \\ &= T^{2\lambda+\hat{m}+k-2} B(\lambda+\hat{m}+k+0.5, \lambda+0.5) \\ &= T^{2\lambda+\hat{m}+k-2} \frac{\Gamma(\lambda+\hat{m}+k+0.5) \Gamma(\lambda+0.5)}{(2\lambda+\hat{m}+k+1)}. \end{aligned} \quad (4.6)$$

Substituting Eq (4.6) in (4.5) gives

$$\begin{aligned} \hat{\xi}_{T,\hat{n}\hat{m}} &= \frac{T^{\hat{m}-2} 2^{4\lambda-1} \hat{n}! (\hat{n} + \lambda) \Gamma^2(\lambda) \Gamma(\lambda + 0.5)}{\pi \Gamma(\hat{n} + 2\lambda)} \\ &\times \sum_{k=0}^{\hat{n}} (-1)^{k+\hat{n}} \frac{\Gamma(k + 2\lambda + \hat{n}) \Gamma(k + \lambda + \hat{m} - 0.5)}{k! (\hat{n} - k - 1)! \Gamma(k + \lambda + 0.5) \Gamma(k + 2\lambda + \hat{m})}. \end{aligned} \quad (4.7)$$

Finally, the desired result can be obtained by changing the indices $m = \hat{m} + 1, n = \hat{n} + 1$ and replacing $\hat{\Theta}_{T,m-1}^T$ and $\hat{\xi}_{T,(m-1)(n-1)}$ by $\Theta_{T,m}^T$ and $\xi_{T,mn}$, respectively. \square

We give an example to illustrate for $\lambda = 1, T = 1$ and $m = 4$.

$$\Theta_{1,4} = \begin{pmatrix} 167/148 & 0 & 0 & 0 & 0 \\ 167/296 & 167/592 & 0 & 0 & 0 \\ 707/2005 & 167/592 & 167/2368 & 0 & 0 \\ 643/2605 & 643/2605 & 437/4131 & 135/7657 & 0 \\ 453/2447 & 373/1763 & 437/3672 & 270/7657 & 135/30628 \end{pmatrix}.$$

Lemma 4.2. *The derivatives of the monomial function vector $\Phi_p(\tau)$ in (4.1) satisfy*

$$\frac{d\Phi_p(\tau)}{d\tau} = \mathbb{D}_p^{(1)} \Phi_p(\tau), \quad (4.8)$$

and

$$\frac{d^r \Phi_p(\tau)}{d\tau^r} = \mathbb{D}_p^{(r)} \Phi_p(\tau), \quad (4.9)$$

in which $\mathbb{D}_p^{(r)}$ represents the r^{th} power of the strictly lower triangular matrix $\mathbb{D}_p^{(1)}$ with

$$\left[\mathbb{D}_p^{(1)} \right]_{mn} = \begin{cases} 0, & m = 1, 1 \leq n \leq p + 1, \\ m - 1, & 2 \leq m \leq p + 1, 1 \leq n \leq p + 1, m - n = 1. \end{cases}$$

Proof. The result of the lemma can be implied by the definitions of vectors $\Phi_p(\tau)$ and $\mathbb{D}_p^{(1)}$. \square

Lemma 4.3. *$\Phi_p(\tau)$ denotes the monomial function vector in (4.1), then*

$$\frac{\partial^{\theta(\sigma,\tau)} \Phi_p(\tau)}{\partial \tau^{\theta(\sigma,\tau)}} = \mathbb{Z}_p^{(\theta(\sigma,\tau))} \Phi_p(\tau), \quad (4.10)$$

with

$$\left[\mathbb{Z}_p^{(\theta(\sigma,\tau))} \right]_{mn} = \begin{cases} 0, & m = 1, 1 \leq n \leq p + 1, \\ \frac{(m-1)! C(\theta(\sigma,\tau))}{1-\theta(\sigma,\tau)} \mathbf{E}_{\theta(\sigma,\tau),m} \left(\frac{-\theta(\sigma,\tau) \tau^{\theta(\sigma,\tau)}}{1-\theta(\sigma,\tau)} \right), & 2 \leq m \leq p + 1, \\ 1, & 1 \leq n \leq p + 1, m = n. \end{cases}$$

Proof. It is easy to complete the proof by using Corollary 2.1. \square

Theorem 4.1. *The derivative of SGPs vector $\Psi_{T,p}(\tau)$ in (3.6) satisfies*

$$\frac{d\Psi_{T,p}(\tau)}{d\tau} = \mathbf{D}_{T,p}^{(1)} \Psi_{T,p}(\tau), \quad (4.11)$$

where $\mathbf{D}_{T,p}^{(1)}$ represents the $(p+1)$ -order operational matrix of the SGPs given by

$$\mathbf{D}_{T,p}^{(1)} = \Theta_{T,p}^{-1} \mathbb{D}_p^{(1)} \Theta_{T,p}.$$

Generally, the r -order derivative of $\Psi_{T,p}(\tau)$ satisfies

$$\frac{d^r \Psi_{T,p}(\tau)}{d\tau^r} = \mathbf{D}_{T,p}^{(r)} \Psi_{T,p}(\tau), \quad (4.12)$$

in which $\mathbf{D}_{T,p}^{(r)}$ represents the r^{th} power of the matrix $\mathbf{D}_{T,p}^{(1)}$.

Proof. It can be proved simply from Eq (4.1) and Lemma 4.2. \square

Theorem 4.2. *The SGPs vector $\Psi_{T,p}(\tau)$ in (3.6) satisfies*

$$\frac{\partial^{\theta(\sigma,\tau)} \Psi_{T,p}(\tau)}{\partial \tau^{\theta(\sigma,\tau)}} = \mathbf{Z}_{T,p}^{(\theta(\sigma,\tau))} \Psi_{T,p}(\tau) \quad (4.13)$$

with

$$\mathbf{Z}_{T,p}^{(\theta(\sigma,\tau))} = \Theta_{T,p}^{-1} \mathbb{Z}_p^{(\theta(\sigma,\tau))} \Theta_{T,p}.$$

Here the $(p+1)$ -order matrix $\mathbf{Z}_{T,p}^{(\theta(\sigma,\tau))}$ is the operator matrix of SGPs in the sense of variable order $\theta(\sigma, \tau)$.

Proof. The proof is completed by using Lemma 4.2 and Eq (4.10). \square

5. Numerical scheme

The unknown solution $u(\sigma, \tau)$ of Eq (1.1) is approximated by the SGPs as follows

$$u(\sigma, \tau) \simeq u_{q,p}(\sigma, \tau) = \sum_{m=0}^q \sum_{n=0}^p u_{mn} G_{X,m}^\lambda(\sigma) G_{T,n}^\lambda(\tau) \triangleq \Psi_{X,q}(\xi)^T \mathbf{U} \Psi_{T,p}(\tau), \quad (5.1)$$

where $\mathbf{U} = [u_{mn}]_{(q+1) \times (p+1)}$ is an unknown matrix, $\Psi_{X,q}(\xi)$ and $\Psi_{T,p}(\tau)$ represent the vectors mentioned in Eq (3.8).

Using Eqs (4.11), (4.12) and (5.1), one has

$$\frac{\partial u(\sigma, \tau)}{\partial \sigma} \simeq \Psi_{X,q}(\sigma)^T (\mathbf{D}_{X,q}^{(1)})^T \mathbf{U} \Psi_{T,p}(\tau), \quad (5.2)$$

and

$$\frac{\partial^2 u(\sigma, \tau)}{\partial \sigma^2} \simeq \Psi_{X,q}(\sigma)^T (\mathbf{D}_{X,q}^{(2)})^T \mathbf{U} \Psi_{T,p}(\tau). \quad (5.3)$$

Moreover, Theorem 4.2 results in

$$\frac{\partial^{\theta(\sigma,\tau)} u(\sigma, \tau)}{\partial \tau^{\theta(\sigma,\tau)}} \simeq \Psi_{X,q}(\xi)^T \mathbf{U} \mathbf{Z}_{T,p}^{(\theta(\sigma,\tau))} \Psi_{T,p}(\tau). \quad (5.4)$$

Combining Eqs (5.1)–(5.4) and (1.1), we have

$$\begin{aligned} \mathbf{R}(\sigma, \tau) \triangleq & \Psi_{X,q}(\sigma)^T \left[\mathbf{U} \mathbf{Z}_{T,p}^{(\theta(\sigma,\tau))} - \kappa \left(\mathbf{D}_{X,q}^{(2)} \right) \mathbf{U} + \lambda \left(\mathbf{D}_{X,q}^{(1)} \right) \mathbf{U} \right] \Psi_{T,p}(\tau) \\ & - \delta \left(\sigma, \tau, \Psi_{X,q}(\sigma)^T \mathbf{U} \Psi_{T,p}(\tau) \right) - f(\sigma, \tau). \end{aligned} \quad (5.5)$$

From the initial and boundary conditions in Eq (1.1) and (5.1), we have

$$\mathbf{M}_1(\sigma) \triangleq \Psi_{X,q}(\sigma)^T \mathbf{U} \Psi_{T,p}(0) - g(\sigma), \quad (5.6)$$

and

$$\begin{aligned} \mathbf{M}_2(\tau) & \triangleq \Psi_{X,q}(0)^T \mathbf{U} \Psi_{T,p}(\tau) - h_1(\tau), \\ \mathbf{M}_3(\tau) & \triangleq \Psi_{X,q}(X)^T \mathbf{U} \Psi_{T,p}(\tau) - h_2(\tau). \end{aligned} \quad (5.7)$$

Finally, Eqs (5.5)–(5.7) are combined to the following system

$$\begin{cases} \mathbf{R}(\sigma_m, \tau_n) = 0, & 2 \leq m \leq q, 2 \leq n \leq p + 1, \\ \mathbf{M}_1(\sigma_m) = 0, & 1 \leq m \leq q + 1, \\ \mathbf{M}_2(\tau_n) = 0, & 2 \leq n \leq p + 1, \\ \mathbf{M}_3(\tau_n) = 0, & 2 \leq n \leq p + 1. \end{cases} \quad (5.8)$$

For solving the unknown matrix \mathbf{U} in the above $(q + 1) \times (p + 1)$ nonlinear algebraic equations, we can choose Gaussian nodes

$$\sigma_m = \frac{X}{2} \left(1 - \cos \left(\frac{(2m - 1)\pi}{2(q + 1)} \right) \right), \quad m = 1, 2, \dots, q + 1$$

and

$$\tau_n = \frac{T}{2} \left(1 - \cos \left(\frac{(2n - 1)\pi}{2(p + 1)} \right) \right), \quad n = 1, 2, \dots, p + 1.$$

Then by substituting \mathbf{U} into Eq (5.1), an approximate solution of Eq (1.1) can be obtained.

6. Numerical examples and results

The effectiveness of the proposed scheme is shown through some numerical simulations. All computations are carried out in MATLAB software. For $i = 1, 2$, let $\varepsilon_i = \max(|u_E^i - u_N^i|)$ be the i -th maximum absolute error (MAE), with u_E^i and u_N^i are the analytical solution and numerical solution, respectively. $\eta_i = (q_i + 1)(p_i + 1)$ represents the number of the SGPs used in the i -th approximations. Then the order of the convergence (CO) corresponding to the approximate solutions is defined by

$$\text{CO} = \log_{\frac{\eta_1}{\eta_2}} \left(\frac{\varepsilon_2}{\varepsilon_1} \right).$$

Example 1. If $\delta(\sigma, \tau, u(\sigma, \tau)) + f(\sigma, \tau) = 0$, then the model (1.1) reduces to [36]

$$\begin{cases} \frac{\partial^{\theta(\sigma, \tau)} u(\sigma, \tau)}{\partial \tau^{\theta(\sigma, \tau)}} = \kappa \frac{\partial^2 u(\sigma, \tau)}{\partial \sigma^2} - \mu \frac{\partial u(\sigma, \tau)}{\partial \sigma}, & (\sigma, \tau) \in [0, 1] \times [0, 1], \\ u(\sigma, 0) = \exp\left\{-\frac{(\sigma - \mu)^2}{4\kappa}\right\}, \\ u(0, \tau) = \frac{1}{\sqrt{1 + \tau}} \exp\left\{-\frac{((1 + \tau)\mu)^2}{4\kappa(1 + \tau)}\right\}, & u(1, \tau) = \frac{1}{\sqrt{1 + \tau}} \exp\left\{-\frac{(1 - (1 + \tau)\mu)^2}{4\kappa(1 + \tau)}\right\}. \end{cases} \quad (6.1)$$

If $\theta(\sigma, \tau) = 1$, the solution of Eq (6.1) reads

$$u(\sigma, \tau) = \frac{1}{\sqrt{1 + \tau}} \exp\left\{-\frac{(\sigma - (1 + \tau)\mu)^2}{4\kappa(1 + \tau)}\right\}.$$

Set $\kappa = 0.1, \mu = 0.25, \lambda = 1$ and $q = 7, p = 7$. Figure 1 shows the numerical results for $u(\sigma, 0.4), u(0.4, \tau)$ for different constant functions $\theta(\sigma, \tau)$. Numerical simulations for $u(\sigma, 0.6), u(0.6, \tau)$ with some values of $\theta(\sigma, \tau)$ are displayed in Figure 2. Comparison of the approximation solution with $\theta(\sigma, \tau) = 0.75 + 0.15\sin(2\pi\sigma\tau)$ and the exact solution with $\theta(\sigma, \tau) = 1$ are depicted in Figure 3. It can be seen that the numerical solutions are convergent. Table 1 compares the absolute errors of the method proposed in this paper (abbreviated as SGPs method) with those obtained in [36] for various choices of $\theta(\sigma, \tau)$ and $q = p = 4$ at $t = 0.8$. It is observed that we achieved an excellent approximation for the exact solution. In Table 2, the L_2 errors are presented for $q = p = 6$ and various values $\theta(\sigma, \tau)$ at $x = 0.6$.

Example 2. If $\kappa = 1, \mu = 0$ and $f(\sigma, \tau) = 0$, then the model (1.1) becomes [30]

$$\begin{cases} \frac{\partial^{\theta(\sigma, \tau)} u(\sigma, \tau)}{\partial \tau^{\theta(\sigma, \tau)}} = \frac{\partial^2 u(\sigma, \tau)}{\partial \sigma^2} + u(\sigma, \tau)(1 - u(\sigma, \tau))(u(\sigma, \tau) - \gamma), & (\sigma, \tau) \in [0, 20] \times [0, 1], 0 < \gamma < 1, \\ u(\sigma, 0) = \left(1 + e^{\frac{-\sigma}{\sqrt{2}}}\right)^{-1}, \\ u(0, \tau) = \left(1 + e^{\frac{-1}{\sqrt{2}}\left(\frac{1-2\gamma}{\sqrt{2}}\tau\right)}\right)^{-1}, & u(20, \tau) = \left(1 + e^{\frac{-1}{\sqrt{2}}\left(20 + \frac{1-2\gamma}{\sqrt{2}}\tau\right)}\right)^{-1}. \end{cases} \quad (6.2)$$

One finds that the solution of Eq (6.2) is $u(\sigma, \tau) = \left(1 + e^{\frac{-1}{\sqrt{2}}\left(\sigma + \frac{1-2\gamma}{\sqrt{2}}\tau\right)}\right)^{-1}$ in the case $\theta(\sigma, \tau) = 1$. For $\lambda = 0.5, q = 9, p = 12$, the obtained numerical results of $u(\sigma, 0.2)$ and $u(3, \tau)$ with different constant functions $\theta(\sigma, \tau)$ are shown in Figure 4. Results of some functions $\theta(\sigma, \tau)$ with $\lambda = 1, q = 9, p = 9$ are shown in Figure 5. Comparison of the numerical solution with $\lambda = 1, q = 9, p = 9, \theta(\sigma, \tau) = 0.75 + 0.2 \sin(\sigma\tau)$ and analytical solution with $\lambda = 1, q = 9, p = 9, \theta(\sigma, \tau) = 1$ are depicted in Figure 6. It can be seen that the numerical solutions are convergent.

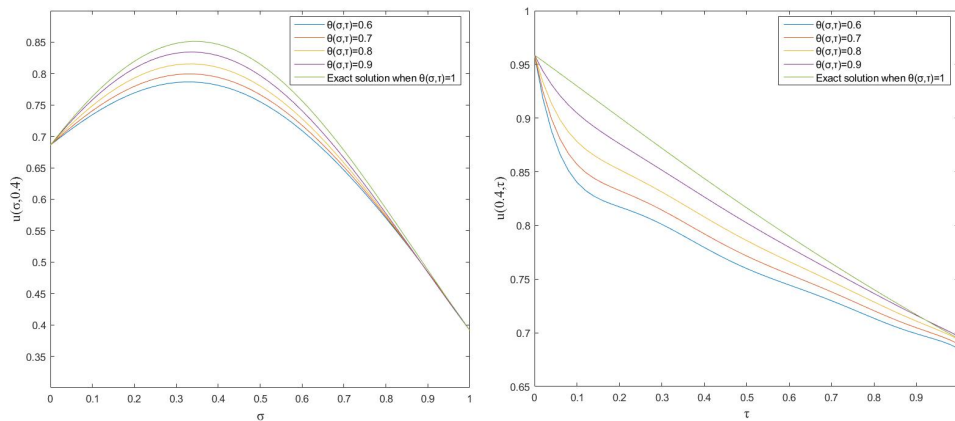


Figure 1. Approximate solutions for various constant functions $\theta(\sigma, \tau)$ when $\tau = 0.4$ (left) and $\sigma = 0.4$ (right) in Example 1.

Table 1. Comparison of the absolute errors between the SGPs method and [36] for various constant functions $\theta(\sigma, \tau)$ and $q = p = 4$ at $t = 0.8$ for Example 1.

x	$\theta(\sigma, \tau) = 0.9$		$\theta(\sigma, \tau) = 0.97$		$\theta(\sigma, \tau) = 0.99$	
	SGPs method	[36]	SGPs method	[36]	SGPs method	[36]
0.0	7.7543e-06	9.1048e-05	7.7543e-06	2.9324e-04	7.7543e-06	2.7498e-04
0.1	4.1764e-03	2.8503e-03	2.1942e-03	1.4968e-03	7.9833e-04	6.3345e-04
0.2	4.5583e-03	2.1194e-03	3.0129e-03	1.4223e-03	1.2540e-03	6.0235e-04
0.3	1.7086e-03	1.4002e-03	2.3432e-03	1.2294e-04	1.0646e-03	2.0999e-05
0.4	3.2240e-03	6.5033e-03	6.2026e-04	1.8748e-03	4.2900e-04	8.2568e-04
0.5	8.9240e-03	1.1885e-02	1.5920e-03	3.9751e-03	3.7131e-04	1.6113e-03
0.6	1.4130e-02	1.6362e-02	3.8215e-03	5.7354e-03	1.1935e-03	2.1911e-03
0.7	1.7624e-02	1.8878e-02	5.6763e-03	6.8670e-03	2.0213e-03	2.6014e-03
0.8	1.7986e-02	1.8271e-02	6.6020e-03	7.0116e-03	2.7225e-03	2.8375e-03
0.9	1.3170e-02	1.2881e-02	5.4550e-03	5.3375e-03	2.6220e-03	2.4489e-03

Table 2. L_2 errors for various choices of $\theta(\sigma, \tau)$ and $q = p = 6$ at $x = 0.6$ for Example 1.

t	$\theta(\sigma, \tau) = 0.65$	$\theta(\sigma, \tau) = 0.75$	$\theta(\sigma, \tau) = 0.85$	$\theta(\sigma, \tau) = 0.95$
0.0	1.7024e-04	1.7024e-04	1.7024e-04	1.7024e-04
0.1	2.1400e-02	1.3067e-02	5.6521e-03	1.6086e-03
0.2	3.5167e-02	2.4885e-02	1.4133e-02	4.4922e-03
0.3	4.2944e-02	3.2616e-02	2.0529e-02	6.8666e-03
0.4	4.6426e-02	3.6283e-02	2.3783e-02	8.2178e-03
0.5	4.6979e-02	3.7017e-02	2.4574e-02	8.6250e-03
0.6	4.5540e-02	3.5991e-02	2.3948e-02	8.3791e-03
0.7	4.2631e-02	3.3851e-02	2.2541e-02	7.7379e-03
0.8	3.8505e-02	3.0675e-02	2.0401e-02	6.8207e-03
0.9	3.3413e-02	2.6451e-02	1.7405e-02	5.6513e-03

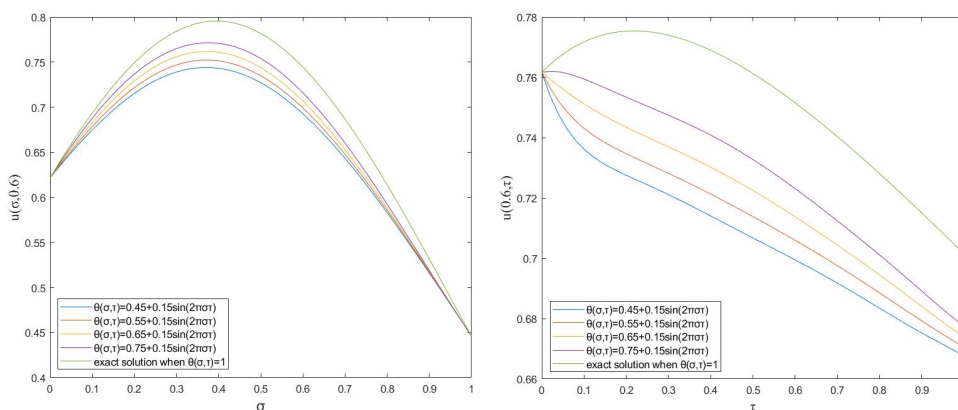


Figure 2. Approximate solutions for various sin functions $\theta(\sigma, \tau)$ when $\tau = 0.6$ (left) and $\sigma = 0.6$ (right) in Example 1.

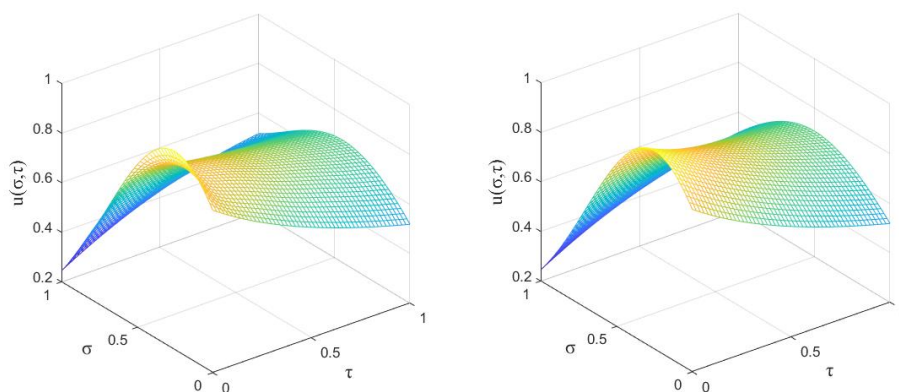


Figure 3. Comparison of the numerical solution ($\theta(\sigma, \tau) = 0.75 + 0.15\sin(2\pi\sigma\tau)$, left) and exact solution ($\theta(\sigma, \tau) = 1$, right) in Example 1.

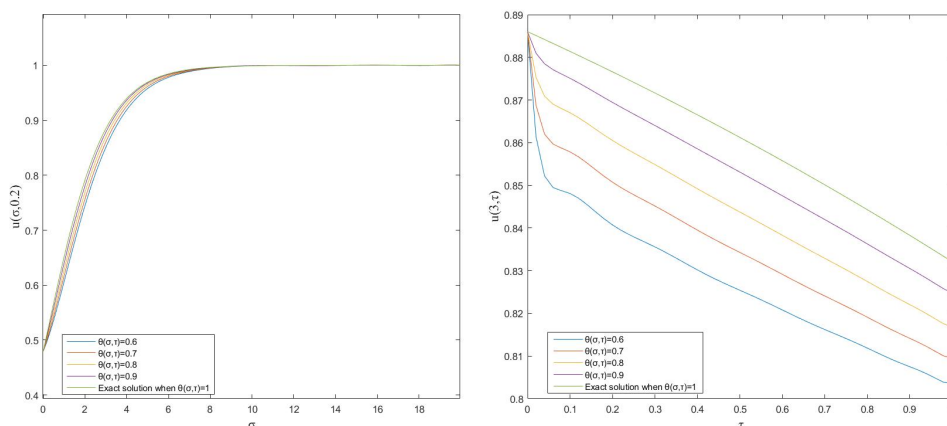


Figure 4. Exact solution and the numerical solutions for some constant functions $\theta(\sigma, \tau)$ when $\tau = 0.2$ (left) and $\sigma = 3$ (right) in Example 2.

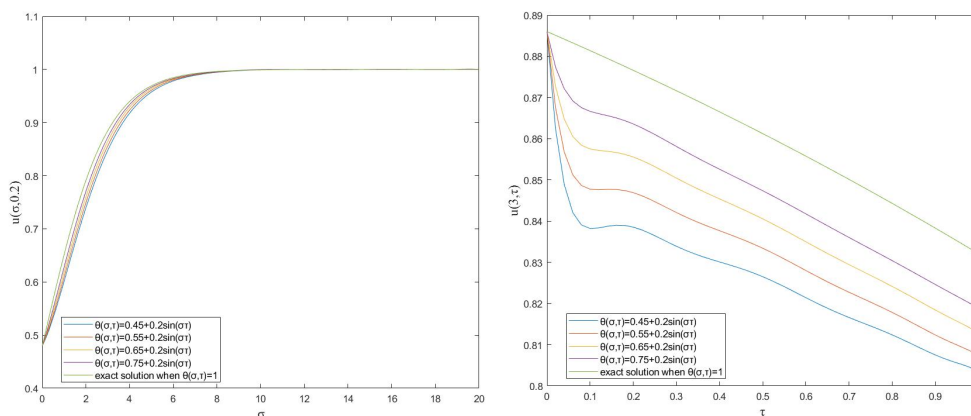


Figure 5. Exact solution and the numerical solutions for various sin functions $\theta(\sigma, \tau)$ when $\tau = 0.2$ (left) and $\sigma = 3$ (right) in Example 2.

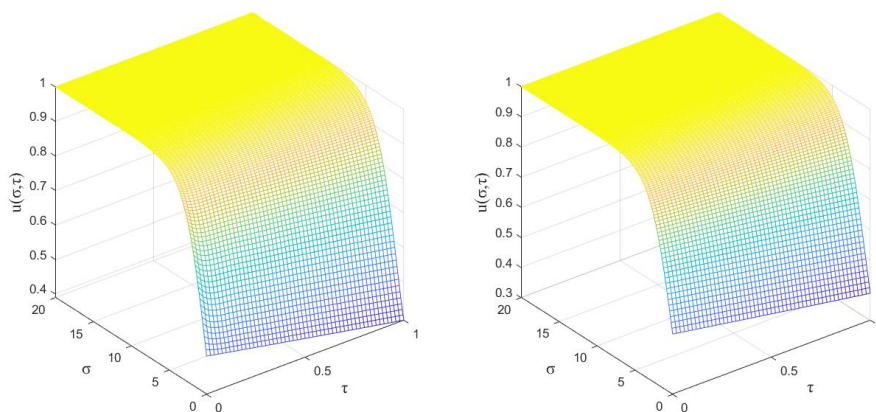


Figure 6. Comparison of the numerical solutions ($\theta(\sigma, \tau) = 0.75 + 0.2\sin(\sigma\tau)$, left) and the exact solution ($\theta(\sigma, \tau) = 1$, right) in Example 2.

In order to compare the results with the works in [30], we discuss the following case

$$\begin{cases} \kappa = 2, \delta(\sigma, \tau, u(\sigma, \tau)) = \sin(u(\sigma, \tau)), g(\sigma) = \left(1 + e^{\frac{-\sigma}{\sqrt{2}}}\right)^{-1}, \\ h_1(\tau) = \left(1 + e^{\frac{-1}{\sqrt{2}}\left(\frac{1-2\gamma}{\sqrt{2}}\tau\right)}\right)^{-1}, h_2(\tau) = \left(1 + e^{\frac{-1}{\sqrt{2}}\left(20 + \frac{1-2\gamma}{\sqrt{2}}\tau\right)}\right)^{-1}, (\sigma, \tau) \in [0, 2] \times [0, 2], \\ f(\sigma, \tau) = \left(\frac{\mathbf{C}(\theta(\sigma, \tau))3!\tau^3}{1 - \theta(\sigma, \tau)} \mathbf{E}_{\theta(\sigma, \tau), 4} \left(\frac{-\theta(\sigma, \tau)\tau^{\theta(\sigma, \tau)}}{1 - \theta(\sigma, \tau)}\right) + 2\tau^3\right) \sin(\sigma) - \sin(\tau^3 \sin(\sigma)). \end{cases} \quad (6.3)$$

The analytical solution of this case is given by $u(\sigma, \tau) = \tau^3 \sin(\sigma)$. This example has been solved for two different functions $\theta(\sigma, \tau)$ by utilizing the presented method (abbreviated as SGPs method) with $p = 3$ and some values of q . In Tables 3 and 4, the MAE errors are listed for the present method (abbreviated as SGPs method) and the method proposed in [30]. It can be seen that the SGPs method is able to achieve smaller errors.

Table 3. Comparison of the MAEs of the SGPs method and [30] for $\theta(\sigma, \tau) = 0.35 + 0.20 \sin(\sigma\tau)$ with $q = 6$ and $q = 8$ for $p = 3$ in (6.3).

(σ, τ)	$\theta(\sigma, \tau) = 0.35 + 0.2 \sin(\sigma\tau)$			
	$q = 6$		$q = 8$	
	SGPs method	[15]	SGPs method	[15]
(0.4,0.4)	7.5142e-09	4.0307e-06	2.0855e-10	6.0803e-08
(0.8,0.8)	1.3277e-06	2.1531e-05	4.0701e-10	1.1765e-07
(1.2,1.2)	1.4326e-06	2.5412e-05	8.6563e-09	1.0783e-07
(1.6,1.6)	1.2779e-07	2.6078e-05	2.8258e-08	1.1608e-07
(2.0,2.0)	1.5072e-05	0.0000e-00	8.0406e-08	0.0000e-00

Table 4. Comparison of the MAEs of the SGPs method and [30] for $\theta(\sigma, \tau) = 0.75 + 0.20 \sin(\sigma\tau)$ with $q = 6$ and $q = 8$ for $p = 3$ in (6.3).

(σ, τ)	$\theta(\sigma, \tau) = 0.75 + 0.2 \sin(\sigma\tau)$			
	$q = 6$		$q = 8$	
	SGPs method	[30]	SGPs method	[30]
(0.4,0.4)	1.0110e-08	2.3337e-06	1.3449e-10	3.2104e-10
(0.8,0.8)	1.2079e-06	1.0804e-05	6.3519e-12	4.8010e-08
(1.2,1.2)	1.5555e-06	2.8356e-05	8.3785e-09	1.0948e-07
(1.6,1.6)	4.4606e-07	3.2703e-05	2.7956e-08	1.2767e-07
(2.0,2.0)	1.5071e-05	0.0000e-00	8.0337e-08	0.0000e-00

Example 3. If $\kappa = \mu = 1$ and $f(\sigma, \tau) = 0$, then the model (1.1) is

$$\begin{cases} \frac{\partial^{\theta(\sigma, \tau)} u(\sigma, \tau)}{\partial \tau^{\theta(\sigma, \tau)}} = \frac{\partial^2 u(\sigma, \tau)}{\partial \sigma^2} - \frac{\partial u(\sigma, \tau)}{\partial \sigma} + \delta(\sigma, \tau, u(\sigma, \tau)), & 0 \leq \sigma \leq X, 0 \leq \tau \leq T, \\ u(\sigma, 0) = e^\sigma, \\ u(0, \tau) = e^\tau, \quad u(X, \tau) = e^{\tau+X}. \end{cases} \quad (6.4)$$

Let $\delta(\sigma, \tau, u(\sigma, \tau)) = u(\sigma, \tau) \frac{\partial^2 u(\sigma, \tau)}{\partial \sigma^2} - u(\sigma, \tau)^2 + u(\sigma, \tau)$ and $\theta(\sigma, \tau) = 1$, then the solution of Eq (6.4) reads $u(\sigma, \tau) = e^{\sigma+\tau}$. When $\lambda = 0.5, X = 0.5, T = 0.5, q = 10, p = 8$, numerical results of $u(\sigma, 0.2)$ and $u(0.2, \tau)$ with constant function $\theta(\sigma, \tau)$ are shown in Figure 7. Comparison of the numerical solution with $\lambda = 1, X = 0.5, T = 1, q = 9, p = 9, \theta(\sigma, \tau) = 0.75 + 0.15 \sin(2\pi\sigma\tau)$ and the analytical solution with $\theta(\sigma, \tau) = 1$ are depicted in Figure 8. It can be seen that the numerical solutions are convergent.

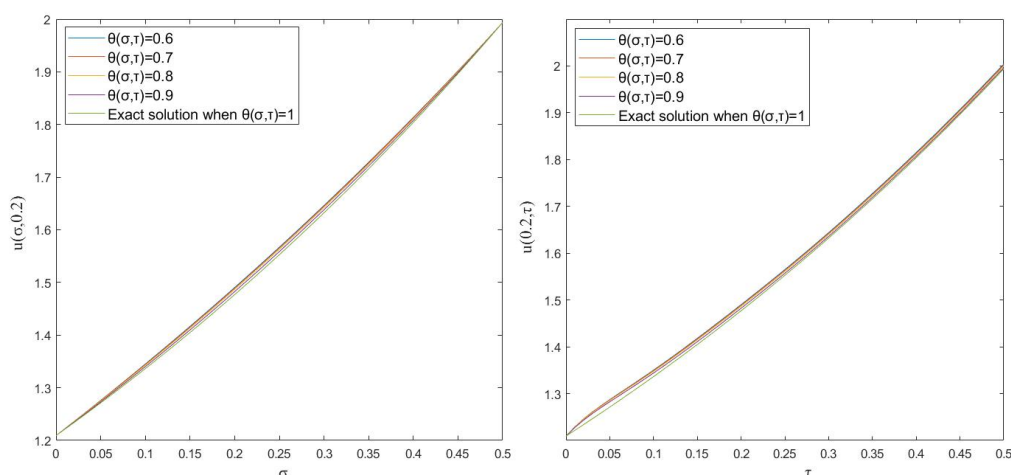


Figure 7. Exact solution and the numerical solutions for some constants when $\tau = 0.2$ (left) and $\sigma = 0.2$ (right) in Example 3.

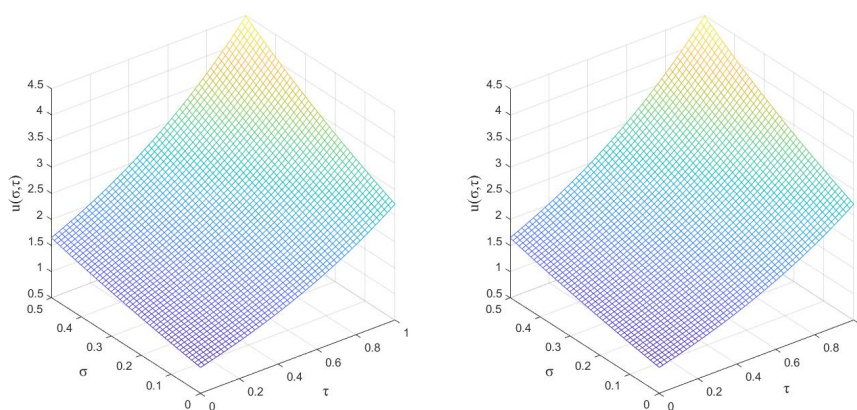


Figure 8. Comparison of the numerical solution ($\theta(\sigma, \tau) = 0.75 + 0.15 \sin(2\pi\sigma\tau)$, left) and exact solution ($\theta(\sigma, \tau) = 1$, right) in Example 3.

Example 4. If $\kappa = \mu = 1$ and $\delta(\sigma, \tau, u(\sigma, \tau)) = 2u(\sigma, \tau)$, then the model (1.1) reads like

$$\begin{cases} \frac{\partial^{\theta(\sigma, \tau)} u(\sigma, \tau)}{\partial \tau^{\theta(\sigma, \tau)}} = \frac{\partial^2 u(\sigma, \tau)}{\partial \sigma^2} - \frac{\partial u(\sigma, \tau)}{\partial \sigma} + 2u(\sigma, \tau) + f(\sigma, \tau), & 0 \leq \sigma \leq X, 0 \leq \tau \leq T, \\ u(\sigma, 0) = \sin(\sigma), \\ u(0, \tau) = 0, u(X, \tau) = \sin(X)e^{-\tau}. \end{cases} \quad (6.5)$$

Given

$$f(\sigma, \tau) = \frac{-C(\theta(\sigma, \tau))\tau \sin(\sigma)}{1 - \theta(\sigma, \tau)} \sum_{k=0}^{\infty} (-\tau)^k E_{\theta(\sigma, \tau), k+2} \left(\frac{-\theta(\sigma, \tau)\tau^{\theta(\sigma, \tau)}}{1 - \theta(\sigma, \tau)} \right) - \sin(\sigma)e^{-\tau} + 0.5 \cos(\sigma)e^{-\tau},$$

the solution of Eq (6.5) is $u(\sigma, \tau) = \sin(\sigma)e^{(-\tau)}$. Comparison of the numerical solution when $X = 0.5, T = 1, \lambda = 1, q = 6, p = 6, \theta(\sigma, \tau) = 0.7 + 0.2\sin(\sigma\tau)$ and the exact solution are depicted in

Figure 9. Table 5 displays the results of the MAEs and CO for different parameters in Example 4. It is clear that the SGP's method has a good convergence rate.

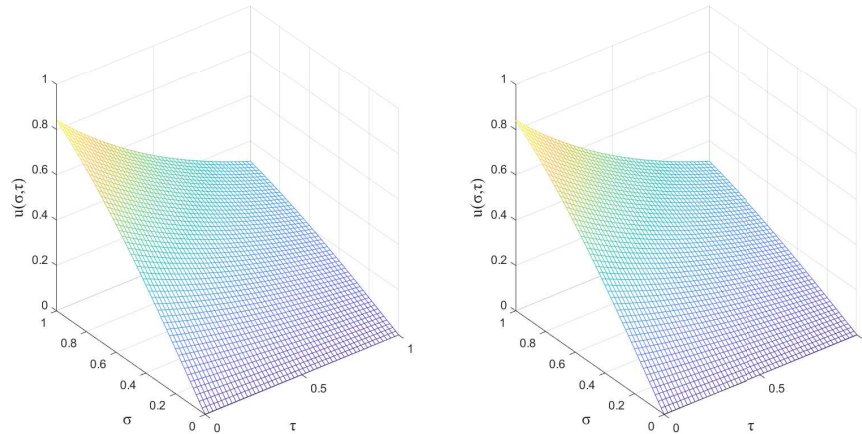


Figure 9. Comparison of the approximate solution ($\theta(\sigma, \tau) = 0.7 + 0.2 \sin(\sigma\tau)$, left) and the exact solution (right) in Example 4.

Table 5. The MAEs, L_2 errors and CO of the SGP's method with some different parameters in Example 4.

q	p	$\lambda=0.5$			$\lambda=1$		
		L_2	MAEs	CO	L_2	MAEs	CO
5	5	1.8456e-05	1.1892E-06	-	1.8456e-05	1.1892E-06	-
6	6	2.4800e-07	5.5076E-08	8.4255	2.4790e-07	5.5079E-08	8.4254
7	7	2.3590e-08	1.3617E-09	12.0013	2.3477e-08	1.3629E-09	11.9984
8	8	1.6077e-10	5.4460E-11	12.0533	9.5183e-10	8.9108E-11	10.2131
q	p	$\lambda=1.5$			$\lambda=2$		
		L_2	MAEs	CO	L_2	MAEs	CO
5	5	1.8456e-05	1.1892E-06	-	1.8456e-05	1.1892E-06	-
6	6	2.4802e-07	5.5075E-08	8.4256	2.4798e-07	5.5077E-08	8.4255
7	7	2.3628e-08	1.3595E-09	12.0065	2.3620e-08	1.3403E-09	12.0526
8	8	8.7781e-11	5.0231E-11	12.3499	3.0124e-09	1.4625E-10	8.2952

Example 5. If $\kappa = \mu = 1$ and $\delta(\sigma, \tau, u(\sigma, \tau)) = 0$, then the model (1.1) is

$$\begin{cases} \frac{\partial^{\theta(\sigma, \tau)} u(\sigma, \tau)}{\partial \tau^{\theta(\sigma, \tau)}} = \frac{\partial^2 u(\sigma, \tau)}{\partial \sigma^2} - \frac{\partial u(\sigma, \tau)}{\partial \sigma} + f(\sigma, \tau), & (\sigma, \tau) \in [0, 1] \times [0, 1], \\ u(\sigma, 0) = 0, & u(0, \tau) = u(1, \tau) = 0. \end{cases} \quad (6.6)$$

For force function

$$f(\sigma, \tau) = 120 \frac{C(\theta(\sigma, \tau))}{1 - \theta(\sigma, \tau)} \tau^5 \sin \pi \sigma \times E_{\theta(\sigma, \tau), 6} \left[\frac{-\theta(\sigma, \tau)}{1 - \theta(\sigma, \tau)} \tau^{\theta(\sigma, \tau)} \right] + (\pi \sin(\pi \theta(\sigma, \tau)) + \cos(\pi \theta(\sigma, \tau))),$$

the solution of Eq (6.6) reads $u(\sigma, \tau) = \tau^5 \sin \pi \sigma$. Comparison of the numerical solution when $\lambda = 1.2$, $q = 14$, $p = 9$, $\theta(\sigma, \tau) = 0.8 - 0.2e^{-2\sigma\tau}$ and the exact solution are displayed in Figure 10. It can be seen that the numerical solution is convergent.

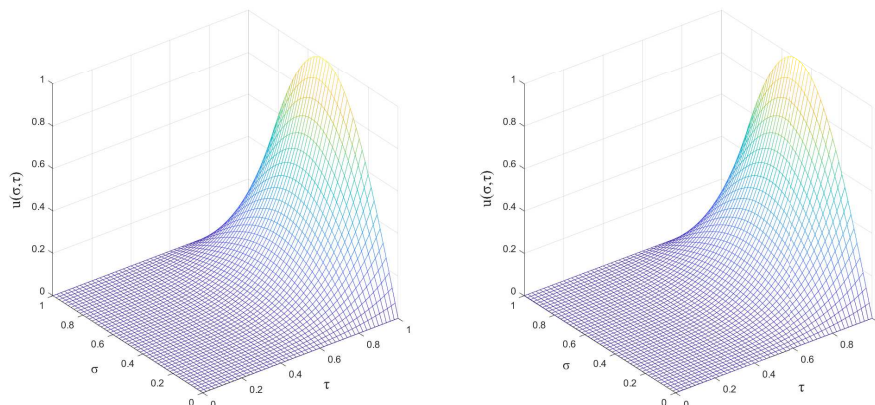


Figure 10. Comparison of the approximate solution ($\theta(\sigma, \tau) = 0.8 - 0.2e^{-2\sigma\tau}$, left) and the exact solution (right) in Example 4.

Finally, we try to use the proposed computational method to solve another type problem.

Example 6. Consider the VO fractional burgers equation [37]

$$\begin{cases} \frac{\partial^{\theta(\sigma, \tau)} u(\sigma, \tau)}{\partial \tau^{\theta(\sigma, \tau)}} = V \frac{\partial^2 u(\sigma, \tau)}{\partial \sigma^2} - u(\sigma, \tau) \frac{\partial u(\sigma, \tau)}{\partial \sigma} + f(\sigma, \tau), & 0 < \sigma < X, 0 < \tau < T, \\ u(\sigma, 0) = \sin(2\pi\sigma), & u(0, \tau) = u(1, \tau) = 0. \end{cases} \quad (6.7)$$

It is hard to find the analytical solution of Eq (6.7) with ABC fractional derivative, but we are able to predict by the proposed method simultaneously the solutions with ordinary and variable fractional derivative with some initial parameters. Choose $X = 1$, $T = 5$, numerical results of some spatial and time nodes with different $\theta(\sigma, \tau)$ are shown in Figures 11 and 12 respectively. Choose $\lambda = 0.5$, the 3D diagrams of the solutions predicted by the proposed algorithm when $\theta(\sigma, \tau) = 0.4$ and $\theta(\sigma, \tau) = 0.75 + 0.2\sin(2\sigma\tau)$ respectively are shown in Figure 13. It is clear that the numerical solution is convergent.

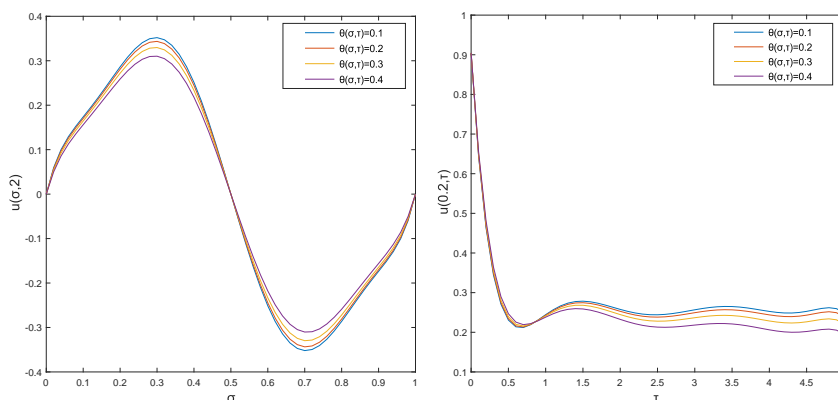


Figure 11. Exact solution and the numerical solutions for various constant functions $\theta(\sigma, \tau)$ when $\tau = 2$ (left) and $\sigma = 0.2$ (right) in Example 6.

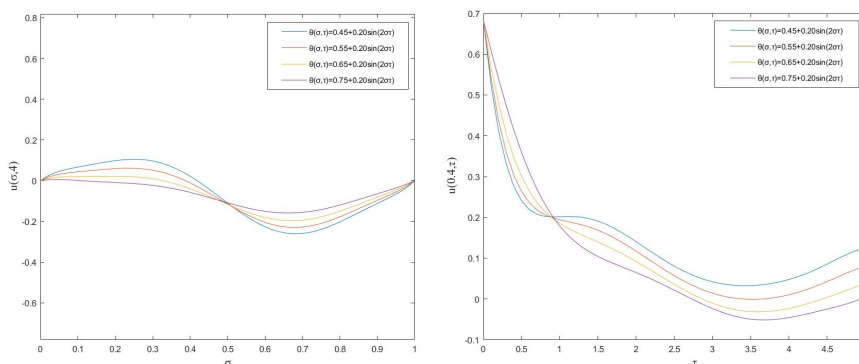


Figure 12. Exact solution and the numerical solutions for some $\theta(\sigma, \tau)$ when $\tau = 4$ (left) and $\sigma = 0.4$ (right) in Example 6.

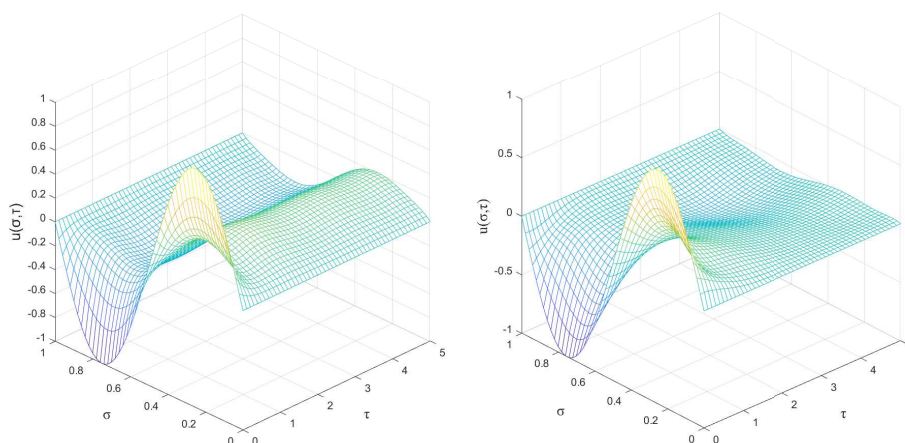


Figure 13. Numerical solutions when $\theta(\sigma, \tau) = 0.4$ ($\lambda = 0.5$, left) and $\theta(\sigma, \tau) = 0.75 + 0.2\sin(2\sigma\tau)$ ($\lambda = 0.5$, right) in Example 6.

7. Conclusions

Shifted orthogonal polynomials combined with spectral methods (such as Galerkin method, collocation method and tau method) can transform complex variable fractional differential equations into algebraic equations, so as to reduce the complexity and improve the accuracy. We propose a numerical approach to solve a VO time fractional model for advection-reaction-diffusion equation with Atangana-Baleanu-Caputo derivative via the shifted Gegenbauer polynomial. By using a collocation approach and obtaining the operational matrix, all that remains is to solve a nonlinear equations. Some examples are given to illustrate the effectiveness of the proposed numerical algorithm.

Acknowledgments

This work was supported by National Natural Science Foundation of China (No. 11971094).

Conflict of interest

The authors declare no conflicts of interest.

References

1. M. Caputo, M. Fabrizio, A new definition of fractional derivative without singular kernel, *Progr. Fract. Differ. Appl.*, **1** (2015), 73–85. <http://dx.doi.org/10.12785/pfda/010201>
2. A. Atangana, D. Baleanu, New fractional derivatives with nonlocal and non-singular kernel: Theory and application to heat transfer model, *Therm. Sci.*, **20** (2016), 763–769. <https://doi.org/10.2298/TSCI160111018A>
3. X. J. Yang, H. M. Srivastava, J. A. Tenreiro Machado, A new fractional derivative without singular kernel: Application to the modelling of the steady heat flow, *Therm. Sci.*, **20** (2016), 753–756. <https://doi.org/10.2298/TSCI151224222Y>
4. S. T. Sutar, K. D. Kucche, On nonlinear hybrid fractional differential equations with Atangana-Baleanu-Caputo derivative, *Chaos Soliton. Fract.*, **143** (2021), 110557. <https://doi.org/10.1016/j.chaos.2020.110557>
5. X. M. Gu, H. W. Sun, Y. L. Zhao, X. Zheng, An implicit difference scheme for time-fractional diffusion equations with a time-invariant type variable order, *Appl. Math. Lett.*, **120** (2021), 107270. <https://doi.org/10.1016/j.aml.2021.107270>
6. M. Hassouna, E. H. El Kinani, A. Ouhadan, Global existence and uniqueness of solution of Atangana-Baleanu-Caputo fractional differential equation with nonlinear term and approximate solutions, *Int. J. Differ. Equations*, **2021** (2021), 5675789. <https://doi.org/10.1155/2021/5675789>
7. J. Gómez-Aguilar, R. Escobar-Jiménez, M. López-López, V. Alvarado-Martínez, Atangana-Baleanu fractional derivative applied to electromagnetic waves in dielectric media, *J. Electromagn. Waves Appl.*, **30** (2016), 1937–1952. <https://doi.org/10.1080/09205071.2016.1225521>

8. S. Ullah, M. A. Khan, M. Farooq, Modeling and analysis of the fractional HBV model with Atangana-Baleanu derivative, *Eur. Phys. J. Plus*, **133** (2018), 313. <https://doi.org/10.1140/epjp/i2018-12120-1>
9. O. J. Peter, A. S. Shaikh, M. O. Ibrahim, K. S. Nisar, D. Baleanu, I. Khan, et al., Analysis and dynamics of fractional order mathematical model of covid-19 in Nigeria using Atangana-Baleanu operator, *Comput. Mater. Con.*, **66** (2020), 1823–1848. <http://dx.doi.org/10.32604/cmc.2020.012314>
10. C. F. Lorenzo, T. T. Hartley, Variable order and distributed order fractional operators, *Nonlinear Dyn.*, **29** (2002), 57–98. <https://doi.org/10.1023/A:1016586905654>
11. H. Sun, W. Chen, H. Wei, A comparative study of constant-order and variable-order fractional models in characterizing memory property of systems, *Eur. Phys. J. Spec. Top.*, **193** (2011), 185. <https://doi.org/10.1140/epjst/e2011-01390-6>
12. M. A. Abdelkawy, M. A. Zaky, A. H. Bhrawy, D. Baleanu, Numerical simulation of time variable fractional order mobile-immobile advection-dispersion model, *Rom. Rep. Phys.*, **67** (2015), 773–791.
13. C. Canuto, M. Y. Hussaini, A. Quarteroni, T. A. Zang, *Spectral methods in fluid dynamics*, Springer, Berlin, 1987.
14. J. Solís-Pérez, J. Gómez-Aguilar, A. Atangana, Novel numerical method for solving variable-order fractional differential equations with power, exponential and Mittag-Leffler laws, *Chaos Soliton. Fract.*, **114** (2018), 175–185. <https://doi.org/10.1016/j.chaos.2018.06.032>
15. X. Li, Y. Gao, B. Wu, Approximate solutions of Atangana-Baleanu variable order fractional problems, *AIMS Math.*, **5** (2020), 2285–2294. <https://doi.org/10.3934/math.2020151>
16. M. H. Heydari, Z. Avazzadeh, A. Atangana, Shifted Jacobi polynomials for nonlinear singular variable-order time fractional Emden-Fowler equation generated by derivative with non-singular kernel, *Adv. Differ. Equations*, **2021** (2021), 188. <https://doi.org/10.1186/s13662-021-03349-1>
17. A. H. Bhrawy, M. A. Zaky, Numerical simulation for two-dimensional variable-order fractional nonlinear cable equation, *Nonlinear Dyn.*, **80** (2015), 101–116. <https://doi.org/10.1007/s11071-014-1854-7>
18. T. El-Gindy, H. Ahmed, M. Melad, Shifted Gegenbauer operational matrix and its applications for solving fractional differential equations, *J. Egypt. Math. Soc.*, **26** (2018), 72–90. <https://doi.org/10.21608/JOMES.2018.9463>
19. M. Usman, M. Hamid, T. Zubair, R. U. Haq, W. Wang, M. Liu, Novel operational matrices-based method for solving fractional-order delay differential equations via shifted Gegenbauer polynomials, *Appl. Math. Comput.*, **372** (2020), 124985. <https://doi.org/10.1016/j.amc.2019.124985>
20. F. Soufivand, F. Soltanian, K. Mamehrashi, An operational matrix method based on the Gegenbauer polynomials for solving a class of fractional optimal control problems, *Int. J. Industrial Electron. Control Optim.*, **4** (2021), 475–484. <https://doi.org/10.22111/IECO.2021.39546.1371>

21. M. Heydari, A. Atangana, A cardinal approach for nonlinear variable-order time fractional schrödinger equation defined by Atangana-Baleanu-Caputo derivative, *Chaos Soliton. Fract.*, **128** (2019), 339–348. <https://doi.org/10.1016/j.chaos.2019.08.009>
22. Y. V. Mukhartova, M. A. Davydova, N. F. Elansky, O. V. Postilyakov, S. A. Zakharova, A. N. Borovski, On application of nonlinear reaction-diffusion-advection models to simulation of transport of chemically-active impurities, *Remote Sensing Technologies and Applications in Urban Environments IV*, **11157** (2019), 180–187. <https://doi.org/10.1117/12.2535489>
23. F. Heße, F. A. Radu, M. Thullner, S. Attinger, Upscaling of the advection-diffusion-reaction equation with Monod reaction, *Adv. Water Resour.*, **32** (2009), 1336–1351. <https://doi.org/10.1016/j.advwatres.2009.05.009>
24. A. Hamdi, Identification of point sources in two-dimensional advection-diffusion-reaction equation: Application to pollution sources in a river. Stationary case, *Inverse Probl. Sci. Eng.*, **15** (2007), 855–870. <https://doi.org/10.1080/17415970601162198>
25. A. Rubio, A. Zalts, C. El Hasi, Numerical solution of the advection-reaction-diffusion equation at different scales, *Environ. Modell. Softw.*, **23** (2008), 90–95. <https://doi.org/10.1016/j.envsoft.2007.05.009>
26. K. Issa, B. M. Yisa, J. Biazar, Numerical solution of space fractional diffusion equation using shifted Gegenbauer polynomials, *Comput. Methods Differ. Equations*, **10** (2022), 431–444. <https://dx.doi.org/10.22034/cmde.2020.42106.1818>
27. U. Ali, A. Iqbal, M. Sohail, F. A. Abdullah, Z. Khan, Compact implicit difference approximation for time-fractional diffusion-wave equation, *Alex. Eng. J.*, **61** (2022), 4119–4126. <https://doi.org/10.1016/j.aej.2021.09.005>
28. M. A. Zaky, S. S. Ezz-Eldien, E. H. Doha, J. A. Tenreiro Machado, A. H. Bhrawy, An efficient operational matrix technique for multidimensional variable-Order time fractional diffusion equations, *ASME J. Comput. Nonlinear Dyn.*, **11** (2016), 061002. <https://doi.org/10.1115/1.4033723>
29. M. M. Izadkhah, J. Saberi-Nadjafi, Gegenbauer spectral method for time-fractional convection-diffusion equations with variable coefficients, *Math. Methods Appl. Sci.*, **38** (2015), 3183–3194. <https://doi.org/10.1002/mma.3289>
30. M. H. Heydari, A. Atangana, Z. Avazzadeh, M. R. Mahmoudi, An operational matrix method for nonlinear variable-order time fractional reaction-diffusion equation involving Mittag-Leffler kernel, *Eur. Phys. J. Plus*, **135** (2020), 237. <https://doi.org/10.1140/epjp/s13360-020-00158-5>
31. P. Pandey, S. Kumar, J. Gómez-Aguilar, Numerical solution of the time fractional reaction-advection-diffusion equation in porous media, *J. Appl. Comput. Mech.*, **8** (2022), 84–96. <https://doi.org/10.22055/JACM.2019.30946.1796>
32. S. Kumar, D. Zeidan, An efficient Mittag-Leffler kernel approach for time-fractional advection-reaction-diffusion equation, *Appl. Numer. Math.*, **170** (2021), 190–207. <https://doi.org/10.1016/j.apnum.2021.07.025>
33. K. S. Miller, B. Ross, *An introduction to the fractional calculus and fractional differential equations*, New York: Wiley, 1993.

34. M. Hosseininia, M. H. Heydari, Legendre wavelets for the numerical solution of nonlinear variable-order time fractional 2d reaction-diffusion equation involving Mittag-Leffler non-singular kernel, *Chaos Soliton. Fract.*, **127** (2019), 400–407. <https://doi.org/10.1016/j.chaos.2019.07.017>
35. F. R. Lin, H. Qu, A Runge-Kutta Gegenbauer spectral method for nonlinear fractional differential equations with Riesz fractional derivatives, *Int. J. Comput. Math.*, **96** (2018), 417–435. <https://doi.org/10.1080/00207160.2018.1487059>
36. H. Tajadodi, A numerical approach of fractional advection-diffusion equation with Atangana-Baleanu derivative, *Chaos Soliton. Fract.*, **130** (2020), 109527. <https://doi.org/10.1016/j.chaos.2019.109527>
37. S. Yadav, R. K. Pandey, Numerical approximation of fractional Burgers equation with Atangana-Baleanu derivative in Caputo sense, *Chaos Soliton. Fract.*, **133** (2020), 109630. <https://doi.org/10.1016/j.chaos.2020.109630>



AIMS Press

©2022 the Author(s), licensee AIMS Press. This is an open access article distributed under the terms of the Creative Commons Attribution License (<http://creativecommons.org/licenses/by/4.0>)